Back mapping in energy domain

For a given $2n$-th order diagram as obtained in the time domain one can write a set of simple rules which allow to obtain at once the multiple energy integral associated to the Laplace transform of the Kernel.

[1] To each of the fermion lines, assign an energy ω_i, as well as the lead and spin indices α_i, σ_i respectively ($1 \leq i \leq n$).
To each section on the contours, assign the energy of the corresponding state

2nd order

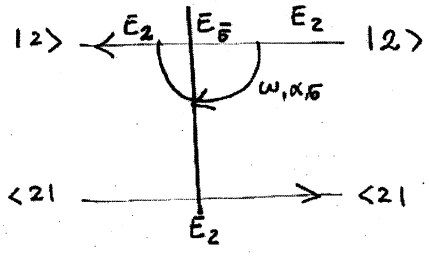

4th order

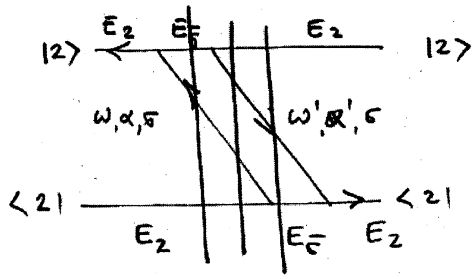

[2] Between two consecutive times τ_j and τ_{j+1} perform a vertical cut. You will obtain $2n-1$ cuts. From each cut obtain a denominator A_j: for each intersection of the cut with a fermion line or a contour, one adds up with a specific sign the energy assigned to the fermion line, respectively to the contour at the intersection. Thereby, the sign is determined by the directions of the fermion line, respectively the contour: If they hit the cut from the right, their energy has to be counted negative, if they come from the left, the sign is positive.

2^{nd} order $\Rightarrow$ $A_0 = E_2 - \omega - E_{\bar\sigma}$

4^{th} order $\Rightarrow$ $A_0 = E_{\bar\sigma} + \omega' - E_2$

$A_1 = E_2 - \omega + \omega' - E_2 = -\omega + \omega'$

$A_2 = E_2 - \omega + E_{\bar\sigma}$

[3] For each fermionic line, determine a sign p_i which tells whether it belongs to an in-tunnelling ($p_i = +$) or an out-tunnelling process ($p_i = -$). Connect to this purpose the two contours at time t, thus obtaining a single oriented contour:

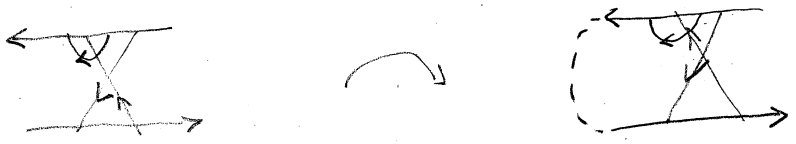

If the fermionic line runs forward with respect to the combined contour $\Rightarrow$ $p_i = -$, if it runs backwards $\Rightarrow$ $p_i = +$.

[4] Determine q, which is the number of vertices on the lower contour plus the number of crossings of fermionic lines

2^{nd} $q = 0 + 0 = 0$

4^{th} $q = 2 + 0 = 2$

[5] Write the final integral

$$-(-1)^q \frac{i}{\hbar} \lim_{\eta \to 0} \prod_{i=1}^{n} \int d\omega_i \, f_{\alpha_i}^{p_i}(\omega_i) \prod_{j=0}^{2n-2} \frac{1}{A_j + i\eta} \qquad (4.48)$$

2^{nd} order $\Rightarrow$ $$-\frac{i}{\hbar} \lim_{\eta \to 0} \int d\omega \, \frac{f_\alpha^-(\omega)}{-\omega + E_2 - E_{\bar\sigma} + i\eta}$$

4^{th} order $\Rightarrow$ $$-\frac{i}{\hbar} \lim_{\eta \to 0} \int d\omega \int d\omega' \, \frac{1}{-\omega + \omega' + i\eta} \, \frac{f_\alpha^+(\omega)}{-\omega + E_2 - E_{\bar\sigma} + i\eta} \, \frac{f_\alpha^-(\omega')}{\omega' - E_2 + E_{\bar\sigma} + i\eta}$$

[6] The tunnelling matrix elements associated to a vertex, $T^{\pm}_{\alpha\sigma}(b,a)$ has a superscript $\pm = \pm$ depending on the creation/annihilation character of the vertex. The subscript $\alpha\sigma$ indicate the lead and the spin quantum number of the electron in the tunnelling event. The arguments a and b to represent the state - with respect of the contour alignment - before and after the vertex respectively.

As an example we calculate one element of the Laplace transform of the Kernel for the Anderson impurity model, both in the 2nd and 4th order contribution in the tunnelling Hamiltonian.

The system Hamiltonian reads:

$$\hat{H}_{sys} = \sum_{\sigma=\uparrow,\downarrow} \varepsilon_\sigma \hat{n}_\sigma + U \hat{n}_\uparrow \hat{n}_\downarrow \qquad (4.49)$$

with the corresponding eigenvectors/eigenvalues: $|0\rangle, 0$; $|\sigma\rangle$ ε_σ ; $|2\rangle$, $\varepsilon_\uparrow + \varepsilon_\downarrow + U = E_2$. The matrix elements that we calculate are $\left(\tilde{K}^{(2)}\right)^{22}_{22}$ and $\left(\tilde{K}^{(4)}\right)^{22}_{22}$. Let's start with the 2nd order:

$$\left(\tilde{K}^{(2)}\right)^{22}_{22} = \sum_\sigma \Bigg(\begin{array}{c} |2\rangle \xleftarrow{\ \sigma\ \sigma\ } |2\rangle \\ \langle 2| \longrightarrow \langle 2| \end{array} + \begin{array}{c} |2\rangle \longleftarrow |2\rangle \\ \langle 2| \xrightarrow{\ \sigma\ \sigma\ } \langle 2| \end{array} \Bigg) \qquad (4.50)$$

Only 2 of the 8 diagrams composing the Kernel $K^{(2)}$ give a finite contribution, due to the particular choice of the initial and final state. Following the prescription of the diagrams in the time domain

$$\left(\tilde{K}^{(2)}\right)^{22}_{22} = -\lim_{\lambda\to 0^+} \sum_\sigma \int_0^\infty d\tau' \, e^{-\lambda\tau'} \langle \hat{C}^-_{3\sigma} \hat{C}^+_{0\sigma} \rangle \langle 2| \hat{D}^+_{3\sigma} \hat{D}^-_{0\sigma} |2\rangle\langle 2|2\rangle + c.c.$$

$$= -\sum_{\sigma\sigma'} \lim_{\lambda\to 0^+} \int_0^\infty d\tau' \, e^{-\lambda t'} \langle \hat{C}^-_{3\sigma} C^+_{0\sigma} \rangle \langle 2| \hat{D}^+_{3\sigma} |\sigma'\rangle\langle\sigma'| \hat{D}^+_{0\sigma} |2\rangle + c.c.$$

(4.49)

$$= -\frac{1}{\hbar^2}\sum_{\sigma\sigma'}\lim_{\lambda\to 0^+}\int_0^\infty d\tau'\, e^{-\lambda\tau'}\sum_{\alpha\vec{k}} f_\alpha^-(\omega_{\vec{k}})\, e^{-i\omega_{\vec{k}}/\hbar\,\tau'}\cdot$$

$$\cdot\langle 2|\, t_{\alpha\vec{k}\sigma}\, t^*_{\alpha\vec{k}'\sigma'}\, e^{iE_2 t/\hbar}\, d^+_{\bar{\sigma}}\,|\sigma'\rangle\langle\sigma'|\, e^{-iE_{\sigma'}t/\hbar}\, e^{iE_{\sigma'}(t-\tau')/\hbar}\, d_\sigma\, e^{-\frac{i}{\hbar}E_2(t-\tau')}|2\rangle$$

$$+ \text{c.c.}$$

$$= -\frac{1}{\hbar^2}\sum_{\alpha\sigma}\lim_{\lambda\to 0^+}\int d\omega\, f_\alpha^-(\omega)\int_0^\infty d\tau'\, e^{-\lambda\tau'}\, e^{-\frac{i}{\hbar}(\omega+E_{\bar{\sigma}}-E_2)\tau'}\, T^+_{\alpha\sigma}(2,\bar{\sigma})\, T^-_{\alpha\sigma}(\bar{\sigma},2)$$

$$+ \text{c.c.}$$

$$= -\frac{1}{\hbar^2}\,\frac{1}{i/\hbar}\lim_{\lambda\to 0^+}\sum_{\alpha\sigma}\int d\omega\, f_\alpha^-(\omega)\,\frac{1}{\omega + E_{\bar{\sigma}} - E_2 - i\lambda}\,\left|T^+_{\alpha\sigma}(2,\bar{\sigma})\right|^2 + \text{c.c.}$$

$$= -\frac{i}{\hbar}\sum_{\alpha\sigma}\left|T^+_{\alpha\sigma}(2,\bar{\sigma})\right|^2\lim_{\lambda\to 0}\int d\omega\,\frac{f_\alpha^-(\omega)}{-\omega + E_2 - E_{\bar{\sigma}} + i\lambda} + \text{c.c.} \qquad (4.51)$$

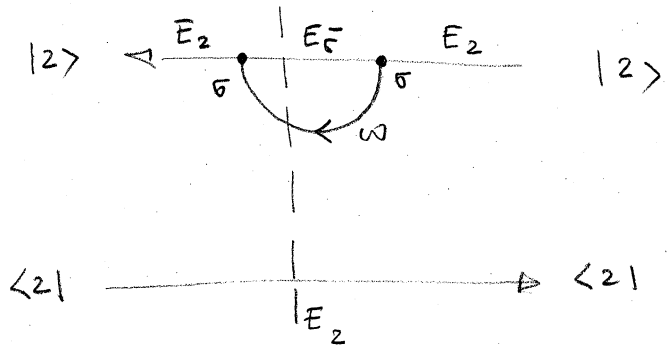

The integral in (4.51) can be calculated with the help of the residual theorem. It yields:

$$\left(K^{(2)}\right)^{22}_{22} = -\frac{2\pi}{\hbar}\sum_{\alpha\sigma}\left|T^+_{\alpha\sigma}(2,\bar{\sigma})\right|^2 f^-(E_2 - E_{\bar{\sigma}} - \mu_\alpha) \qquad (4.52)$$

Now we want to address the 4th order contribution to the same element of the time-evolution kernel:

$$\left(\tilde{K}^{(4)}\right)^{zz}_{zz} =$$

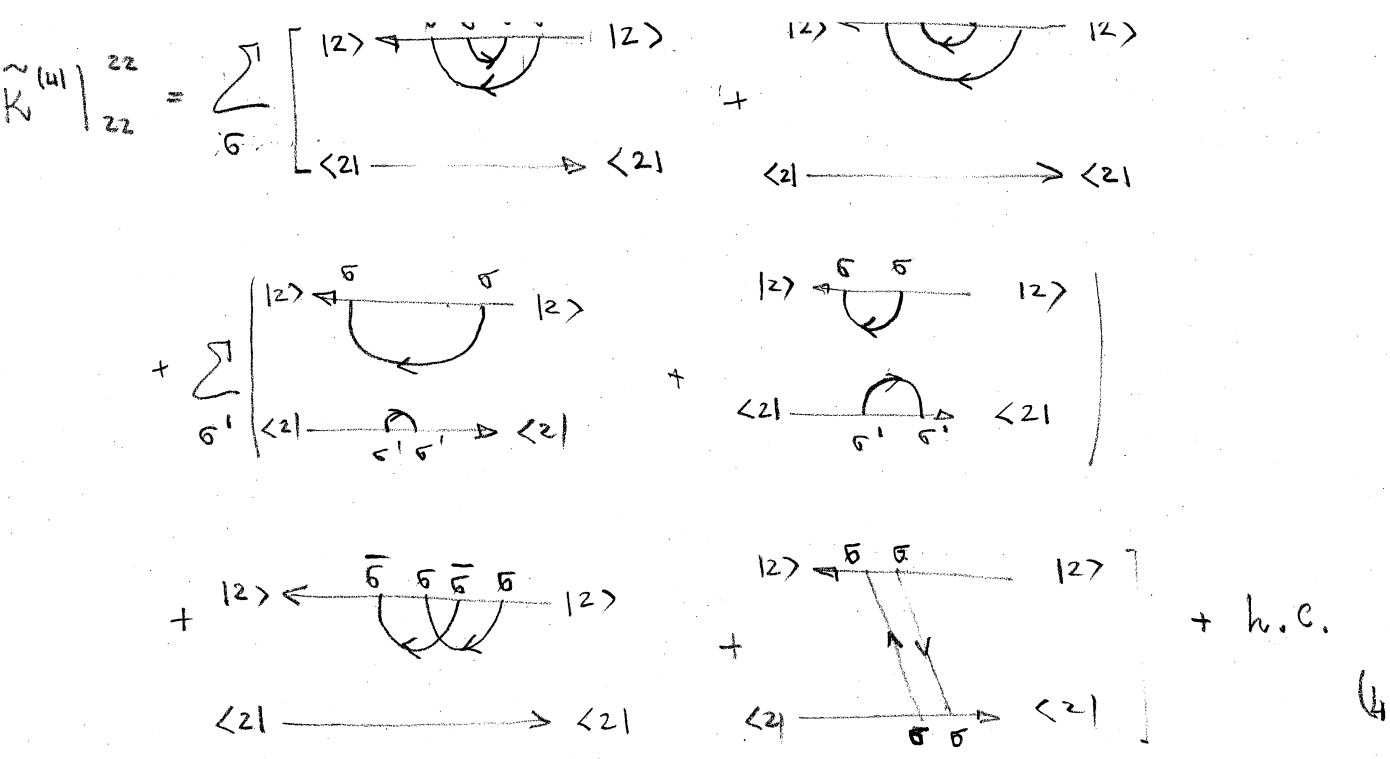

$$+ \bar{\sigma}\,\sigma\,\bar{\sigma}\,\sigma + \text{h.c.} \qquad (4.53)$$

The rules for extracting the 6 diagrams above out of the 16 classes listed at page 111 are

(i) - each contour should have an even number of vertices paired into in and out ones.

(ii) - the first vertex along the contour orientation must be an out-going one, for each of the contours

(iii) - if the second vertex is out-going (in-going) it must be of opposite (equal) spin with respect to the first one.

Rule (i) excludes half of the 4th order diagrams. Rule (ii) excludes the three (classes of) crossed diagrams  . Eventually rule (iii) fixes the orientation of the fermionic lines of the remained 5 classes and leaves "only" the diagrams listed above.

Exemplarily we calculate the last contribution

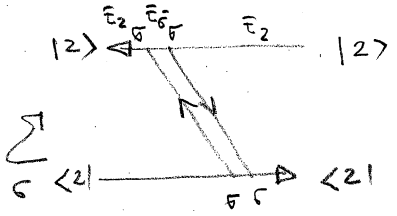

$$= \lim_{\lambda\to 0} \sum_\sigma \int_0^\infty d\tau_2' \, e^{-\lambda\tau_2'} \int_0^{\tau_2'} d\tau_1' \int_0^{\tau_1'} d\tau_2' \, \langle \hat{C}^+_{1\sigma} \hat{C}^-_{3\sigma} \rangle \langle \hat{C}^-_{0,3} \hat{C}^+_{2,\sigma} \rangle$$

$$\langle 2| \hat{D}^+_{3,\sigma} |\bar{\sigma}\rangle\langle\bar{\sigma}| \hat{D}^-_{2\sigma} |2\rangle\langle 2| \hat{D}^+_{0\sigma} |\bar{\sigma}\rangle\langle\bar{\sigma}| \hat{D}^-_{1,\sigma} |2\rangle + \text{c.c.}$$

$$= \frac{1}{\hbar^4} \lim_{\eta\to 0} \sum_{\alpha\alpha'\sigma} \int_0^\infty d\tau_2' \int_{\tau_2'}^\infty d\tau_1' \int_{\tau_1'}^\infty d\tau' \int d\omega \int d\omega' \; f^+_\alpha(\omega) f^-_{\alpha'}(\omega')$$

$$e^{\frac{i}{\hbar}(-\omega + \varepsilon_2 - \bar{\varepsilon}_{\bar{\sigma}})\tau_1'} \; e^{\frac{i}{\hbar}(-\omega' + \varepsilon_2 - \bar{\varepsilon}_{\bar{\sigma}})\tau_2'} \; e^{\frac{i}{\hbar}(\omega' - \varepsilon_2 + \bar{\varepsilon}_{\bar{\sigma}} + i\eta)\tau'}$$

$$T^+_{\alpha\sigma}(2,\bar{\sigma}) \; T^-_{\alpha'\bar{\sigma}}(\bar{\sigma},2) \; T^+_{\alpha'\sigma}(2,\bar{\sigma}) \; T^-_{\alpha,\sigma}(\bar{\sigma},2) \quad + \text{c.c.}$$

$$= -\frac{i}{\hbar} \lim_{\eta\to 0} \sum_{\alpha\alpha'\sigma} \int d\omega \int d\omega' \; f^+_\alpha(\omega) f^-_{\alpha'}(\omega') \left| T^+_{\alpha\sigma}(2,\bar{\sigma}) \right|^2 \left| T^+_{\alpha'\bar{\sigma}}(2,\bar{\sigma}) \right|^2$$

$$\frac{1}{-\omega + \omega' + i\eta} \; \frac{1}{-\omega + \bar{\varepsilon}_2 - \bar{\varepsilon}_{\bar{\sigma}} + i\eta} \; \frac{1}{\omega' - \bar{\varepsilon}_2 + \bar{\varepsilon}_{\bar{\sigma}} + i\eta} + \text{c.c.} \qquad (4.54)$$

where, for the evaluation of the time ordered integration, in the last step, the variable transformations $\tilde{\tau}_2 = \tau_2' - \tau_2'$, $\tilde{\tau} = \tau' - \tau_1'$ which decouples the three time integrals, were applied.

The integrals in (4.69) have an analytical solution calculated using the residual integrals. Interestingly, all the 4th order diagrams reduce to expressions involving only 2 types of functions

$$S\, X^{pp'}_{dd'}(\mu,\mu',\Delta) \quad \text{and} \quad S\, \Delta^{pp'}_{dd'}(\mu,\mu',\Delta)$$

where $S, p, p', d, d' = \pm$

where

$$ {}^{s}\chi^{pp'}_{dd'}(\mu,\mu',\Delta) = \frac{\beta}{ih}\lim_{\eta\to 0}\int dx\int dx'\; f^{p}(x)\, f^{p'}(x') \;\times $$

$$ \times \frac{1}{d(x-\mu)+i\eta}\;\frac{1}{dx+d'x'-\Delta+i\eta}\;\frac{1}{d(sx'-\mu')+i\eta} \qquad (4.55) $$

and

$$ {}^{s}D^{pp'}_{dd'}(\mu,\mu',\Delta) = \frac{\beta}{ih}\lim_{\eta\to 0}\int dx\int dx'\; f^{p}(x)\, f^{p'}(x') \;\times $$

$$ \times \frac{1}{d(x-\mu)+i\eta}\;\frac{1}{dx+d'x'-\Delta+i\eta}\;\frac{1}{d(sx-\mu')+i\eta} \qquad (4.56) $$

Interestingly, the Liouville space approach will reveal that there are formally only 2 classes of diagrams associated to the 2 functions above.

4.2.4 Diagrammatic representation of K_c

The reaction kernel due to non-secular terms reads

$$ \tilde{K}_c = -\tilde{K}^{(2)}_{sn}\,(K_0)^{-1}_{nn}\,\tilde{K}^{(2)}_{ns} $$

This kernel can be seen as a sum of REDUCIBLE fourth order diagrams

Specifically, let's consider the most generic reducible 4th order graph

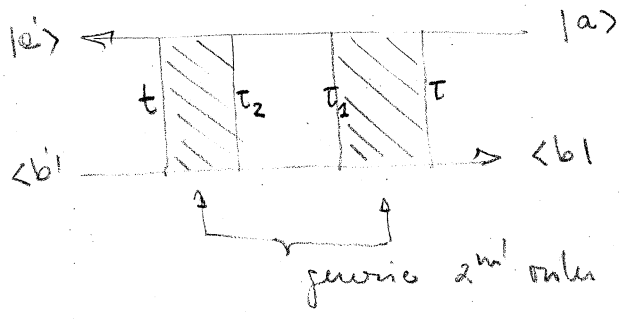

The diagram above can be translated into the analytic expression

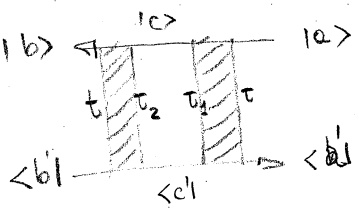

$$= \sum_{cc'} \langle b|U_0(t,0)| \int_0^t d\tau_2\, K_I^{(2)}(t,\tau_2) \left[U_0^+(\tau_2,0) \int_0^{\tau_2} d\tau_1\, U_0(\tau_2,\tau_1)|c\rangle \right.$$

$$\langle c|U_0(\tau_1,0) \int_0^{\tau_1} d\tau\, K_I^{(2)}(\tau_1,\tau) \left[U_0^+(\tau,0)|a\rangle\langle a'|U_0(\tau,0)\right] U_0^+(\tau_1,0)|c'\rangle$$

$$\left. \langle c'|U_0^+(\tau_2,\tau_1)\, U_0(\tau_2,0)\right] U_0^+(t,0)|b'\rangle \qquad (4.57)$$

where one recognizes a sequence of nested operations:

i) $|a\rangle\langle a'| \longrightarrow U_0^+(\tau,0)|a\rangle\langle a'|U_0(\tau,0)$ Schr. to interaction picture

ii) $\int_0^{\tau_1} d\tau\, K_I^{(2)}(\tau_1,\tau)[\quad]$ application of 2nd order Kernel in interaction picture.

iii) $U_0(\tau_1,0)[\quad]U^+(\tau_1,0)$ Interaction to Schr. picture at time τ_1

iv) $\int_0^{\tau_2} d\tau_1\, U_0(\tau_2,\tau_1)[\quad]U_0^+(\tau_2,\tau_1)$ Evolution in the Schr. picture from τ_1 to τ_2

The integral simply ensures that one integrates over all possible cases.

v) $U_0^+(\tau_2,0)[\quad]U_0(\tau_2,0)$ Schr. → interaction picture at time τ_2

vii) $\int_0^t d\tau_2\, K_I^{(2)}(t,\tau_2)[\quad]$ application of the 2nd order Kernel in I picture

viii) $U_0(t,0)[\quad]U_0^+(t,0)$ Back to Schr. picture at time t.

Considering only the Schr. picture

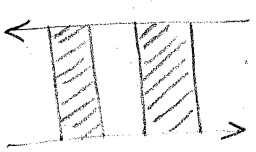

$$= \langle b| \int_0^t d\tau_2\, K^{(2)}(t-\tau_2) \left[\int_0^{\tau_2} d\tau_1\, U_0(\tau_2-\tau_1) \int_0^{\tau_1} d\tau\, K^{(2)}(\tau_1-\tau) \left[|a\rangle\langle a'|\right] U_0^+(\tau_2-\tau_1)\right]$$

(4.58)

that is, 3 convoluted operations on the operator $|a\rangle\langle a'|$. In Laplace space they will then result into the product of operations

$$\tilde{K}^{aa'}_{bb'} = \sum_{\substack{cc' \\ dd'}} \tilde{K}^{(2)\,cc'}_{bb'}\, \tilde{G}^{\,bl\,dd'}_{0\,cc'}\, \tilde{K}^{(2)\,aa'}_{dd'}$$

where, in order to obtain the identification of K_0^{nl}

$$\tilde{g}_0^{nl\ dd'}_{\ cc'} = \lim_{\lambda\to 0} \int_0^\infty d\tau\ e^{-\lambda\tau} \langle c|U_0(\tau,0)|d\rangle\langle d'|U_0^\dagger(\tau,0)|c'\rangle$$

$$= \lim_{\lambda\to 0} \int_0^\infty d\tau\ \delta_{cd}\delta_{d'c'}\ e^{-\frac{i}{\hbar}(E_d - E_{d'})\tau - \lambda\tau} = -\frac{\hbar}{i}\frac{1}{E_{d'} - E_d}\delta_{cd}\delta_{c'd'}$$

(4.59)

in other terms $\left(\tilde{g}_0^{nl}\right)^{dd'}_{cc'} = -\left(\left(K_0\right)^{dd'}_{cc'}\right)^{-1}$.

Notice that the calculated non-local kernel also follows from the diagrammatic rules in energy space

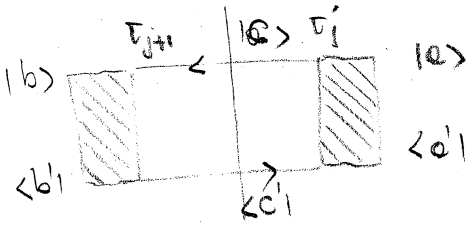

has an extra contribution $-\frac{i}{\hbar}\frac{1}{E_c - E_{c'}}$

The prefactor $-\frac{\hbar}{i}$ of the analytical calculation is needed to compensate the excess of $-\frac{i}{\hbar}$ factors from the 2 2nd order Kernels.

Notice: the nl diagram does not diverge since it is only considered for states with different energies

4.3 Fourth order GME: physical interpretation

The first physical property which can be extracted from the diagrammatic analysis is the probability conservation. $\sum_a \rho_{red,aa}(t) = 1$ $\forall t$ which ensures that the physical system is in a certain state at every moment. A direct consequence $\sum_b \rho_{red,bb} = 0$. The stationary limit of the GME reads:

$$0 = -\frac{i}{\hbar} \sum_{aa'} \delta_{ab}\delta_{a'b'}(E_a - E_{a'}) \rho^{stat}_{aa'} + \sum_{aa'} \tilde{K}^{aa'}_{bb'} \rho^{stat}_{aa'}$$

If we take $b' = b$ we obtain thus the sum rule for the Kernel:

$$\left(\sum_b \tilde{K}^{aa'}_{bb} \right) = 0 \qquad \forall aa' \qquad (4.60)$$

Notice that (4.60) ensures that a non-trivial solution $\rho^{stat}_{aa'}$ exists but the trace condition makes it unique. Eq. (4.60), with $a = a'$ suppose the existence of gain-loss pairs which balance each other.

4.3.1 Gain-loss pairs

Let us consider once again the AIM and restrict ourselves to the case of non-polarized or parallel polarized leads, such that spin coherences can be excluded and we can restrict to populations only.

The GME assumes the form:

$$
\begin{cases}
\dot{P}_0 = -\underbrace{\left(\sum_\sigma \Gamma^{0\to\sigma} + \Gamma^{0\to 2}\right)}_{\tilde{K}^{00}_{00}} P_0 + \sum_\sigma \underbrace{\Gamma^{\sigma\to 0}}_{\tilde{K}^{\sigma\sigma}_{00}} P_\sigma + \underbrace{\Gamma^{2\to 0}}_{\tilde{K}^{22}_{00}} P_2 \\
\dot{P}_\sigma = -\underbrace{\left(\Gamma^{\sigma\to 0} + \Gamma^{\sigma\to\bar{\sigma}} + \Gamma^{\sigma\to 2}\right)}_{\tilde{K}^{\sigma\sigma}_{\sigma\sigma}} P_\sigma + \underbrace{\Gamma^{0\to\sigma}}_{\tilde{K}^{00}_{\sigma\sigma}} P_0 + \underbrace{\Gamma^{\bar{\sigma}\to\sigma}}_{\tilde{K}^{\bar{\sigma}\bar{\sigma}}_{\sigma\sigma}} P_{\bar{\sigma}} + \underbrace{\Gamma^{2\to\sigma}}_{\tilde{K}^{22}_{\sigma\sigma}} P_2 \\
\dot{P}_2 = -\underbrace{\left(\sum_\sigma \Gamma^{2\to\sigma} + \Gamma^{2\to 0}\right)}_{\tilde{K}^{22}_{22}} P_2 + \sum_\sigma \underbrace{\Gamma^{\sigma\to 2}}_{\tilde{K}^{\sigma\sigma}_{22}} P_\sigma + \underbrace{\Gamma^{0\to 2}}_{\tilde{K}^{00}_{22}} P_0
\end{cases}
\qquad (4.61)
$$

Where $P_{0/\sigma/2}$ is the probability of occupation of the corresponding AIM eigenstate $|0\rangle, |\sigma\rangle, |2\rangle$. $\Gamma^{\alpha\to\beta}$ is the rate of transfer of the probability from state $|\alpha\rangle$ to $|\beta\rangle$. Below we identify the different components of the Kernel. Notice (4.76) can be interpreted in Markov approx, or alternatively simply the GME up to given perturbative order for the stationary P^{stat}, if LHS = 0. If we write (4.75) for $\alpha\alpha' = 22$

$$
\underbrace{\tilde{K}^{22}_{22}}_{\text{loss for } |2\rangle} = -\underbrace{\left(\tilde{K}^{22}_{00} + \sum_\sigma K^{22}_{\sigma\sigma}\right)}_{\text{gain (for } |0\rangle \text{ and for } |\sigma\rangle) \text{ from } |2\rangle} \qquad (4.62)
$$

The Kernel element $\tilde{K}^{22}_{22}$ enters in (4.76) as a depopulating rate for state $|2\rangle$. $\tilde{K}^{22}_{00}$ populates $|0\rangle$ from $|2\rangle$ and $\tilde{K}^{22}_{\sigma\sigma}$ populates $|\sigma\rangle$ from $|2\rangle$. This relation is valid at each order. In particular, for 2nd order $\left(\Gamma^{(2)}\right)^{2\to 0} = \left(\tilde{K}^{(2)}\right)^{22}_{00} = 0$

$$
\left(K^{(2)}\right)^{22}_{22} = \sum_\sigma \left(\text{loop: } |2\rangle \leftarrow \sigma, \sigma \leftarrow |2\rangle \text{ and } \langle 2| \rightarrow \langle 2| \right) + \left(|2\rangle \leftarrow |2\rangle \text{ and } \langle 2| \rightarrow \langle 2| \text{ with } \sigma, \sigma \right) \qquad (4.63)
$$

$$
\left(K^{(2)}\right)^{22}_{\sigma\sigma} = \left(|\sigma\rangle \leftarrow \bar{\sigma} \leftarrow |2\rangle \text{ and } \langle\sigma| \rightarrow \bar{\sigma} \rightarrow \langle 2| \right) + \left(|\sigma\rangle \leftarrow \bar{\sigma} \leftarrow |2\rangle \text{ and } |\sigma\rangle \rightarrow \bar{\sigma} \rightarrow \langle 2| \right)
$$

We can thus identify easily the gain-loss pairs

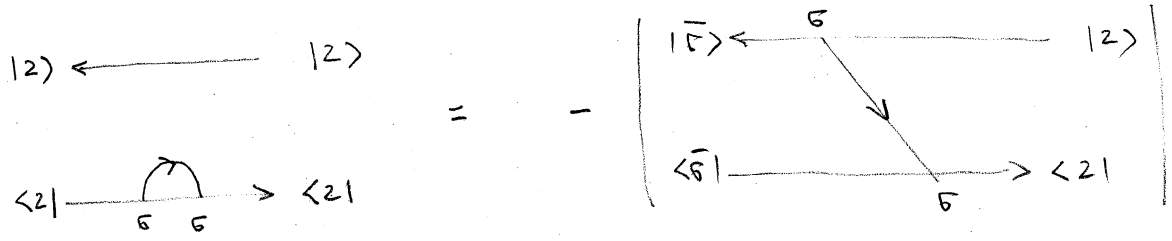

(4.64)

and

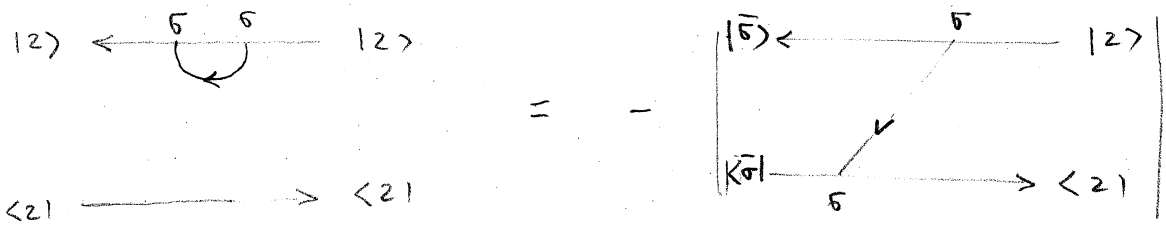

(4.65)

The diagrammatic equations above follow immediately from the diagrammatic rules since a change of contour for the last vertex is associated to a change of sign (no change in the number of fermionic line crossing can happen, to every order). ⇒ gain-loss pairs of diagrams can be easily found to every order by changing the contour of the first or the last vertex.

4.3.2 Fourth order processes

In this section we identify and classify the fourth order processes from a physical point of view: we denote by

co-tunnelling (COT) the contributions where $\Delta N = 0$

cotunnelling assisted sequential tunnelling $\Delta N = \pm 1$

pair tunnelling $\Delta N = \pm 2$

The simple distinction given above should be further complemented with the information that diagrams with a contraction of the first and last time are termed second order diagrams (see last chapter) while the crossed-contractions have no second order counterpart.

Cotunnelling — $\Delta N = 0$

In the AIM we recognize 4 different contributions of cotunnelling processes

$$|0\rangle \to |0\rangle \;,\; |\sigma\rangle \to |\sigma\rangle \;,\; |\sigma\rangle \to |\bar\sigma\rangle \;,\; |2\rangle \to |2\rangle$$

Due to the considerations made above we identify thus the following diagrams:

$\Gamma^{0\to 0}_{cot}$ =

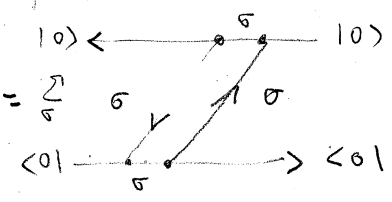

+

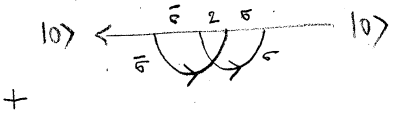

+ h.c.

$\Gamma^{2\to 2}_{cot}$ = $\sum_\sigma$

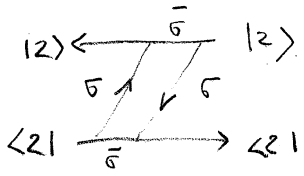

+

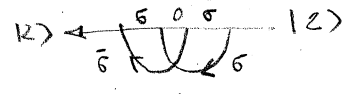

+ h.c.

$\Gamma^{\sigma\to\sigma}_{cot}$ =

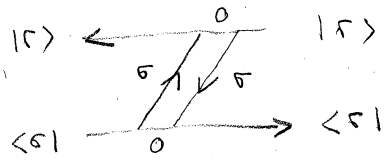

+

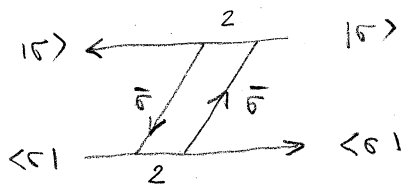

+

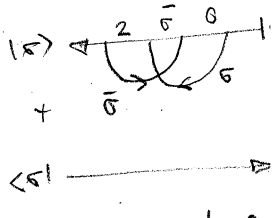

+ h.c.

$\Gamma^{\sigma\to\bar\sigma}_{cot}$ =

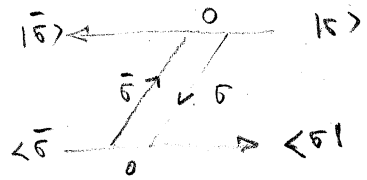

+

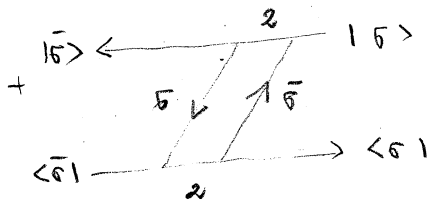

+

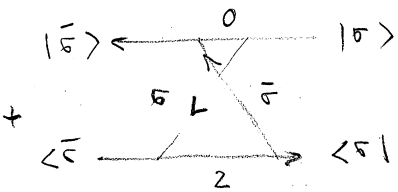

+

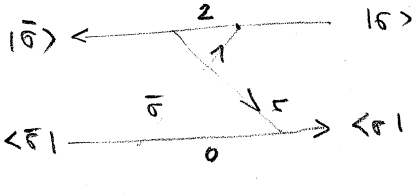

+ h.c.

(4.66)

Each of the terms above has a counterpart in the gain-loss relation in which the particle number varies by 1: exemplarily

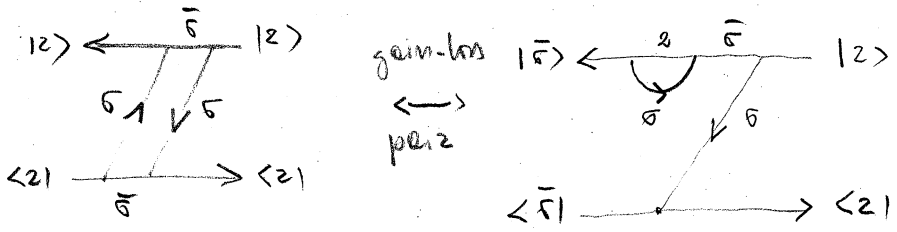

(4.67)

The contributions of cotunnelling are ELASTIC if the initial and final states have the same energy and INELASTIC otherwise (in AIM if $E_\uparrow \neq E_\downarrow$). They give contribution to the conductance. In the first case we obtain a background even at $V_b = 0$. In the second case there is a threshold $eV_b = |E_\uparrow - E_\downarrow|$ which is independent of the gate voltage applied to the system.

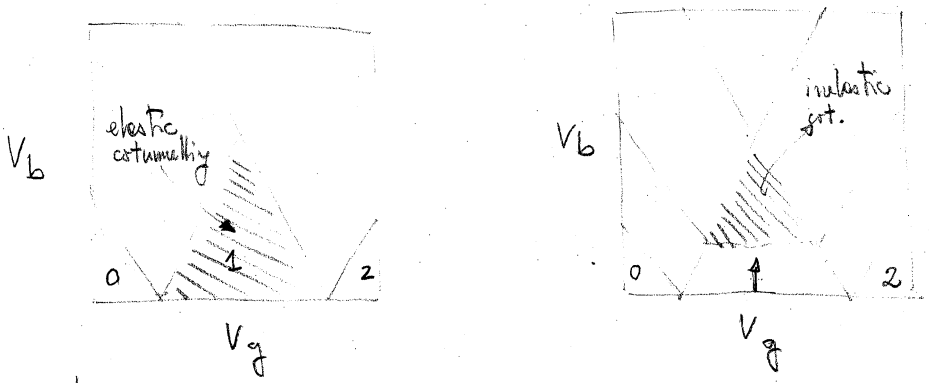

Pair tunnelling $\Delta N = \pm 2$

Again within the "crossed" diagrams we consider the ones associated to the coherent transfer of 2 electrons. We have simply to reverse the sign of one fermionic line in (4.66). We obtain

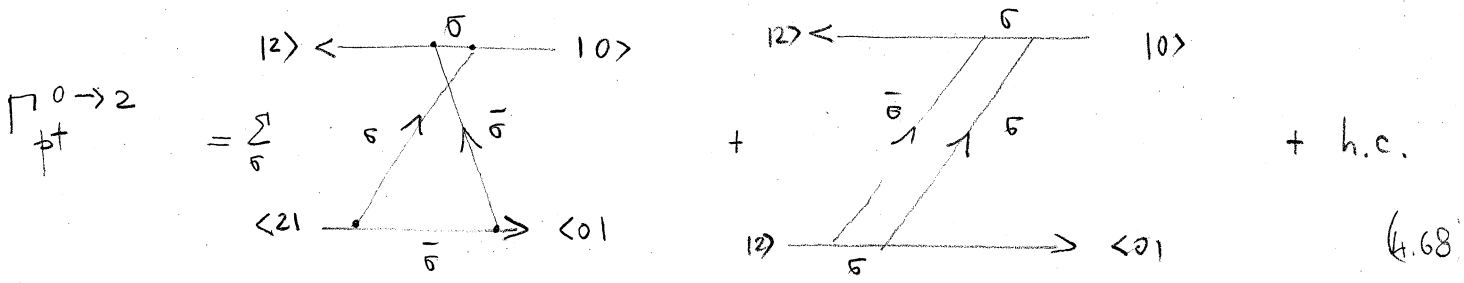

(4.68)

Notice that pair tunnelling processes become energetically allowed at lower biases than the sequential addition/removal $|0\rangle \to |\sigma\rangle \to |2\rangle$ or $|2\rangle \to |\sigma\rangle \to |0\rangle$

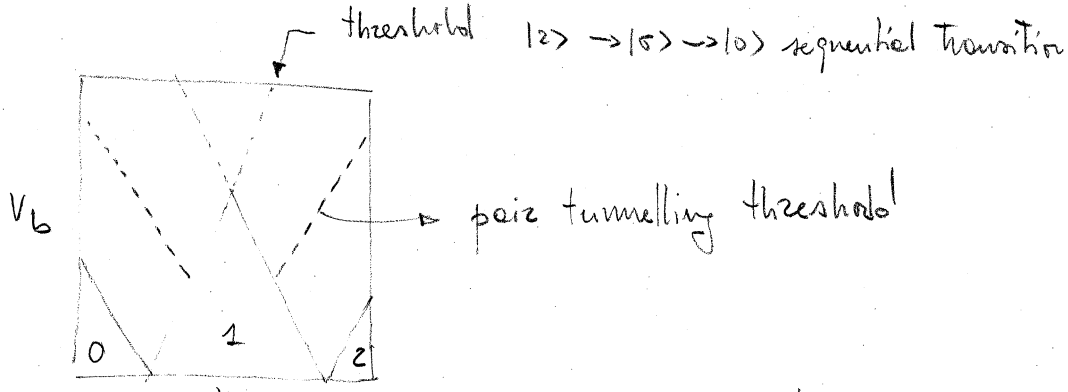

The corresponding transitions $|2\rangle \to |0\rangle$ are given by the graphs:

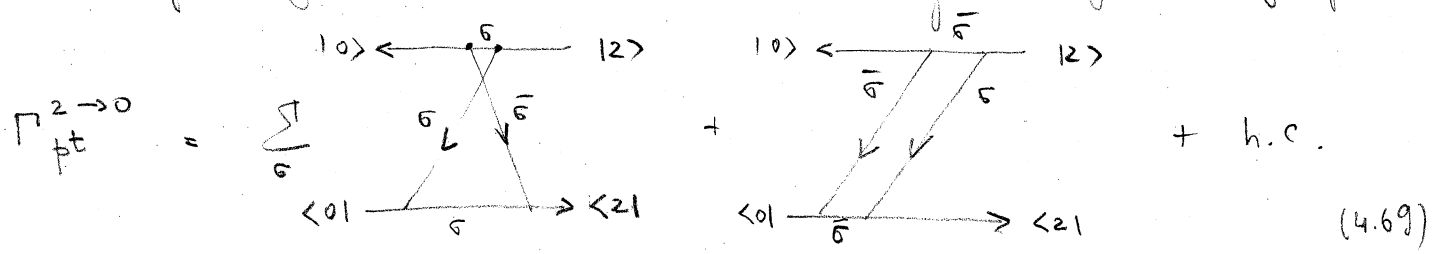

(4.69)

In both cases one can calculate the corresponding gain- loss pairs. For example:

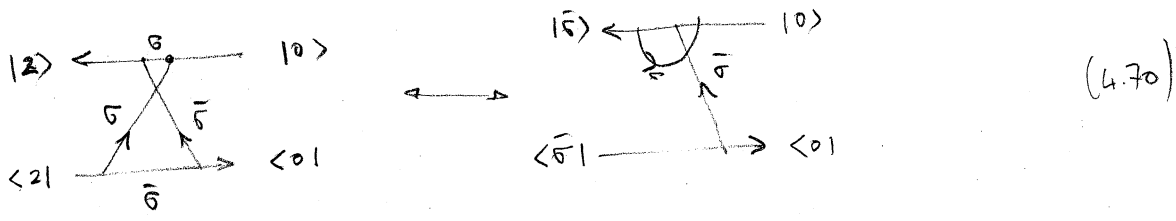

(4.70)

Cotunnelling assisted seq. tunnelling (CO-ST) $\Delta N = \pm 1$

All graphs with even connected leads operators are taken by either COT, PT or by their gain-loss partners. All other graphs correspond to renormalization of sequential tunnelling. For example:

$\Gamma^{0\to\sigma}_{\text{CO-ST}}$ =

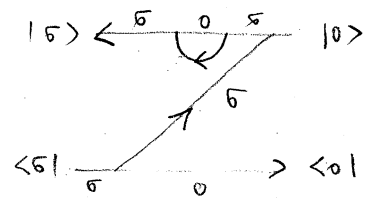

+

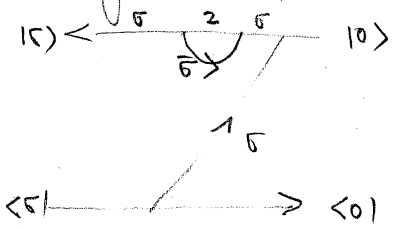

+

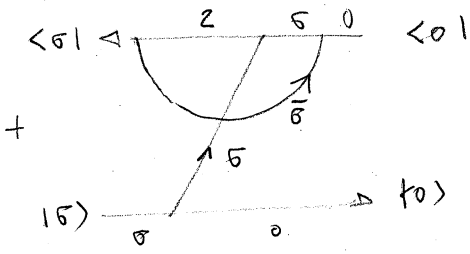

+

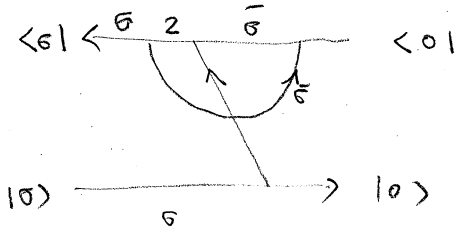

+

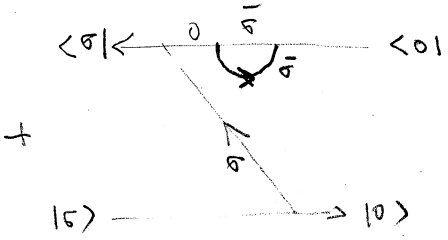

+ h.c. (4.71)

The cotunnelling assisted sequential tunnelling contributes to transport within the cotunnelling regions, but it is gate dependent. In particular, for the inelastic cotunnelling case one can prove: